Assessment of Waveform Control Method for Mitigation of Low-Frequency Current Ripple

G. R. Zhu, H. R. Wang, C. Y. Xiao
Department of Electrical Engineering
Wuhan University of Technology
Wuhan, China
zhgr_55@whut.edu.cn

Siew-Chong Tan
Department of Electrical and
Electronic Engineering,
The University of Hong Kong
Hong Kong

Y. Kang
College of Electrical and
Electronic Engineering
Huazhong University of Sci. and Tech.
Wuhan, China

***Abstract*—Waveform control method can mitigate such a low-frequency ripple current being drawn from the DC distribution while the DC distribution system delivers AC power to the load through a differential inverter. Assessment on the waveform control method and comparative study between with and without waveform control method are proposed in this paper[1]. Experimental results are provided to explain the operation and showcase the performance between with and without the waveform control method. Results validate that the waveform control solution can achieve significant mitigation of the current ripple as well as high quality output voltage without extra hardware. Lower current stress of the switch and higher efficiency can be obtained with waveform control method than without waveform control method.**

I. Introduction

The conversion of DC power into AC power through a single-phase inverter will typically introduce a low-frequency current ripple (at twice the AC output voltage frequency) at the DC input side of the power conversion system. In particular, various passive energy storage compensation methods have been proposed in [1], which involve the incorporation of a large DC capacitor, passive-resonant circuit, or battery at the DC line. The drawback of this approach is that the product size and cost will be increased; On the other hand, it is also possible to mitigate the current ripple through the use of active control methods, e.g. by using dual-loop control [2] or by using a moving-average filter [3]. These methods can achieve only partial mitigation of the low-frequency ripple and generate large overshoots during load transients, which will induce oscillation that will lead to slow dynamic response at the DC bus. Ref. [4] proposed an approach of mitigating low-frequency current ripple of fuel cell power systems through the application of waveform control on differential power inverters, and the waveform control solution can achieve significant mitigation of the current ripple as well as high quality output voltage without extra hardware.

In this paper, a comparative study on the waveform control and the traditional control method without waveform control used in [5], [6], under the same topology, is performed. It will be clearly illustrated in the paper that the waveform control solution achieves significant suppression of the low-frequency current ripple without any additional component, circuit, or electrolytic capacitor, therefore maintaining the overall size and cost. Additionally, the current stress of the switch is decreased and the total efficiency is improved with the use of waveform control.

[1]This research are supported by the National Natural Science Foundation of China (NSFC) number 51107092, University Grants Committee of the Hong Kong Special Administrative Region, Research Grants Council Earmarked Research Grant number PolyU 5283/08E and China Postdoctoral Science Foundation funded project number 2012M511693.

978-1-4673-4355-8/13/$31.00 ©2013 IEEE

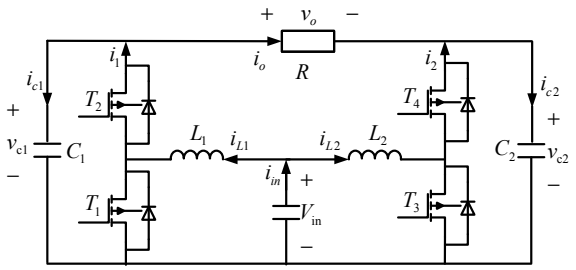

Fig. 1. Schematic of the boost-type differential inverter.

II. DC Distribution Inverter Systems Based on Boost Inverters

A. Overview without waveform control method

A boost-type differential inverter made up of two bi-directional boost converters (see Fig. 1) is adopted as the case study example in the DC distribution system for describing without and with the waveform control method. Here, $V_{\rm in}$ is the DC input voltage, L_1 and L_2 are the power inductors, T_1–T_4 are the power switches, D_1 and D_2 are the free-wheeling diodes, C_1 and C_2 are the output capacitors, and R is the load resistance.

Based upon the boost-type, each converter will generate a DC biased AC output voltage that is higher than the DC voltage of which when the outputs of the two boost converters are combined, only a pure AC output voltage is generated. In conventional practice, a voltage control will be applied on the respective converter to ensure that the output voltage of each converter and their combined output voltage will be respectively

$$v_{\rm c1} = V_{\rm d} + \frac{1}{2}V_{\rm max}\sin(\omega t), \tag{1}$$

$$v_{\rm c2} = V_{\rm d} + \frac{1}{2}V_{\rm max}\sin(\omega t - \pi), \tag{2}$$

$$v_{\rm o} = v_{\rm c1} - v_{\rm c2} = V_{\rm max}\sin(\omega t), \tag{3}$$

where $v_{\rm c1}$ and $v_{\rm c2}$ are the output voltage of the two DC/DC converters, $V_{\rm max}$ is the amplitude of the output voltage $v_{\rm o}$, ω is the line frequency, and $V_{\rm d}$ is the DC-biased voltage of $v_{\rm c1}$ and $v_{\rm c2}$. From (3), it can be observed that the required output is as desired, i.e., comprising only the AC component.

B. Overview with waveform control method

If the capacitor voltages of the two boost converters can be respectively controlled as

$$v_{\rm c1} = V_{\rm d} + \frac{1}{2}V_{\rm max}\sin(\omega t) + B\sin(2\omega t + \varphi), \tag{4}$$

$$v_{\rm c2} = V_{\rm d} + \frac{1}{2}V_{\rm max}\sin(\omega t - \pi) + B\sin(2\omega t + \varphi), \tag{5}$$

then $v_{\rm o}$ will be equivalent to (3). The objective of the waveform control method is to ensure that the capacitor voltages follow precisely (4) and (5).

Since $i = C\frac{dV}{dt}$, the currents of capacitor C_1 and C_2 (for C = C_1 = C_2) can be found from (4) and (5) as

$$i_{\rm c1} = C\omega\frac{1}{2}V_{\rm max}\cos(\omega t) + 2C\omega B\cos(2\omega t + \varphi), \tag{6}$$

$$i_{\rm c2} = -C\omega\frac{1}{2}V_{\rm max}\cos(\omega t) + 2C\omega B\cos(2\omega t + \varphi). \tag{7}$$

Accordingly, from Fig. 1, the inductor currents will be

$$i_{\rm L1} = \frac{(I_{\rm max}\sin(\omega t) + C\omega\frac{1}{2}V_{\rm max}\cos(\omega t) + 2C\omega B\cos(2\omega t + \varphi))v_{\rm c1}}{v_{\rm in}}, \tag{8}$$

$$i_{\rm L2} = \frac{(-I_{\rm max}\sin(\omega t) - C\omega\frac{1}{2}V_{\rm max}\cos(\omega t) + 2C\omega B\cos(2\omega t + \varphi))v_{\rm c2}}{v_{\rm in}}, \tag{9}$$

where d_1 and d_2 are respectively the duty cycles of T_1 and T_3. Therefore, the input current of the inverter, which is the sum of $i_{\rm L1}$ and $i_{\rm L2}$ will be

$$i_{\rm in} = \frac{V_{\rm max}I_{\rm max} + 2B^2C\omega\sin(4\omega t + \varphi) - V_{\rm max}I_{\rm max}\cos(2\omega t)}{2V_{\rm in}} + \frac{\frac{1}{2}V_{\rm max}^2\omega C\sin(2\omega t) + 8V_dBC\omega\cos(2\omega t + \varphi)}{2V_{\rm in}}. \tag{10}$$

From (10), there are three components in the input current $i_{\rm in}$. They are the DC part $\frac{V_{\rm max}I_{\rm max}}{2V_{\rm in}}$, the component at 4ω which is $\frac{2B^2C\omega\sin(4\omega t+\varphi)}{2V_{\rm in}}$, and the low-frequency component at 2ω which is

$$i_{\rm in(2\omega)} = \frac{-V_{\rm max}I_{\rm max}\cos(2\omega t) + \frac{1}{2}V_{\rm max}^2\omega C\sin(2\omega t)}{2V_{\rm in}} + \frac{8V_{\rm d}BC\omega\cos(2\omega t + \varphi)}{2V_{\rm in}}. \tag{11}$$

From (11), it can be seen that if $i_{\rm in(2\omega)}$=0, which means that there will not be a 2ω component in the input current $i_{\rm in}$. Then, amplitude B is derived as

$$B = \frac{V_{\rm max}}{8V_{\rm d}\omega C}\sqrt{I_{\rm max}^2 + \omega^2C^2V_{\rm max}^2/4} \tag{12}$$

and the phase angle φ is derived as

$$\varphi = \frac{\pi}{2} - \sin^{-1}\frac{I_{\rm max}}{\sqrt{I_{\rm max}^2 + \omega^2C^2V_{\rm max}^2/4}}. \tag{13}$$

By ensuring that the capacitor voltages track precisely equations (4) and (5), of which B and φ are calculated from (12) and (13), the low-frequency current ripple of the inverter will be mitigated.

III. Assessment on the Waveform Control Method

A. Flow Path of Double-Line-Frequency Current Component

The flow path of the double-line-frequency current in the power circuit can have a significant impact on the power efficiency and it must be carefully studied. By substituting (12) and (13) into (8) and (9), we have

$$i_{\mathrm{L1w}} = I_D + A_{ww}\sin(\omega t + \theta_1) + A_{3ww}\sin(3\omega t + \theta_3) + A_{4ww}\sin(4\omega t + \theta_4), \quad (14)$$

$$i_{\mathrm{L2w}} = I_D - A_{ww}\sin(\omega t + \theta_1) - A_{3ww}\sin(3\omega t + \theta_3) + A_{4ww}\sin(4\omega t + \theta_4), \quad (15)$$

where i_{L1w} and i_{L2w} are the inductor currents of the inverter with the proposed waveform control, I_D is the DC component of these currents, and the coefficients A_{ww}, A_{3ww} and A_{4ww} are the amplitudes of the fundamental and harmonic components of these currents.

By inspecting the AC components of equations (6), (7), (14) and (15), it is clearly found that with waveform control, the double-line-frequency current component flows mainly through the capacitors C_1 and C_2, and has an insignificant flow through the inductors L_1 and L_2. This is graphically depicted in Fig. 2(a).

On the other hand, without waveform control [5], [6], the expressions of the inductors currents can be derived as

$$i_{\mathrm{L1t}} = I_D + A_{wt}\sin(\omega t + \varphi_1) + A_{2wt}\sin(2\omega t + \varphi_2), \quad (16)$$

$$i_{\mathrm{L2t}} = I_D - A_{wt}\sin(\omega t + \varphi_1) + A_{2wt}\sin(2\omega t + \varphi_2), \quad (17)$$

where the coefficients A_{wt} and A_{2wt} are the amplitudes of the fundamental and harmonic components of the inductor currents.

From (1) and (2), the expressions of the capacitor currents without waveform control can be derived as

$$i_{\mathrm{c1t}} = C\omega\frac{1}{2}V_{\max}\cos(\omega t), \quad (18)$$

$$i_{\mathrm{c2t}} = -C\omega\frac{1}{2}V_{\max}\cos(\omega t). \quad (19)$$

Equations (16), (17), (18), and (19) clearly show that the double-line-frequency current component will mainly flow through L_1 and L_2 instead of C_1 and C_2, as depicted in Fig. 2(b).

Since the inductor is usually a more lossy device (comprising core loss and a higher conductive loss) as compared to the capacitor, it is justify to conclude that the current flow path of the double-line-frequency current given in Fig. 2(b) is more power dissipative than that in Fig. 2(a). Such a conclusion is further verified by the circuit-simulation results given in Fig. 3, which shows the amplitudes of the double-line-frequency current component flowing through each of the main circuit components. From the figure, it is shown that with waveform control, the double-line-frequency current component will mainly flow through C_1, C_2, T_1, T_2, T_3 and T_4 whereas without waveform control, the double-line-frequency current component will mainly flow through T_1, T_3, L_1, L_2 and the DC distribution. This coincides with the theoretical deduction illustrated in Fig. 2. Besides, the double-line-frequency current component flowing through T_1, T_2, T_3 and T_4 will be more balanced with waveform control than that without waveform control.

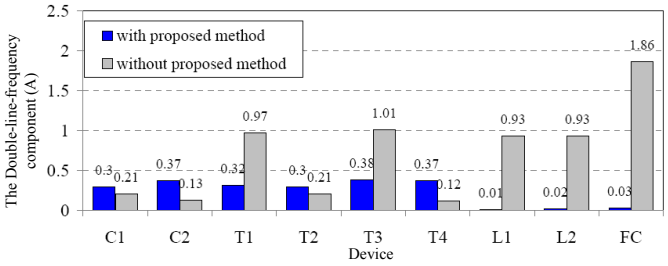

Fig. 3. Amplitude of double-line-frequency current component on the respective power devices.

B. Effect of Capacitance Tolerance

Since the values of the capacitors C_1 and C_2 can affect the computation of the proposed waveform control, the effect of using a difference capacitance from that originally assumed in the computation on the control performance must be investigated. First, the parameters C_1 and C_2 in equations (12) and (13) are chosen as $C_1 = C_2 = 15$ μF for the voltage reference calculation adopted in waveform control. Then, a circuit simulation with C_1 and C_2 in the power stage varied from 5 μF to 25 μF is performed. The simulated results are given in Fig. 4. It is observed that a larger deviation of the capacitor value from the assumed value of 15 μF leads to a poorer compensation of the double-line-frequency component. Yet, as the tolerance of the film capacitor is usually less than 10%, the effect of capacitance tolerance on the compensation capability is small (less than 8.19%), as given in Fig. 4.

IV. Experimental Results and Discussions between with and without Waveform Control Method

A. Control Block and Experimental Setup

To validate the proposed waveform control method, the boost differential inverter prototype as shown in Fig. 1 was implemented.

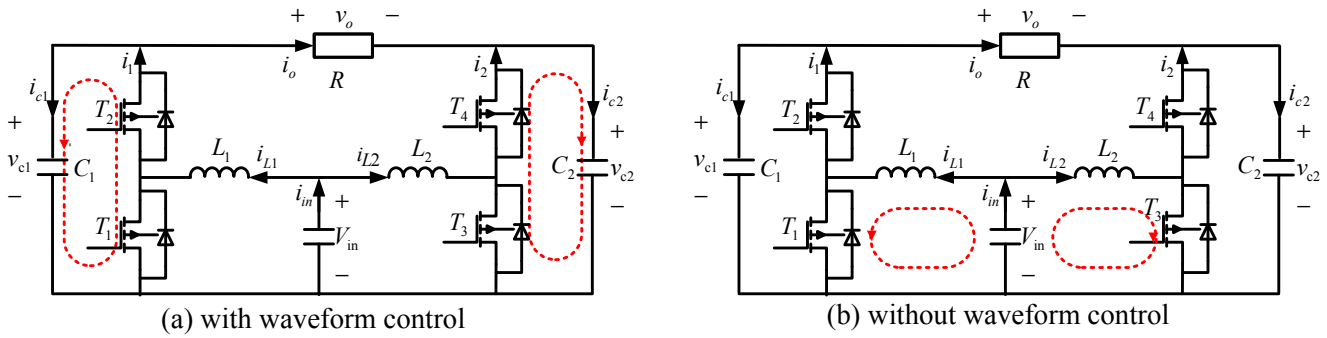

Fig. 2. Flow path of the double-line-frequency current component of the inverter.

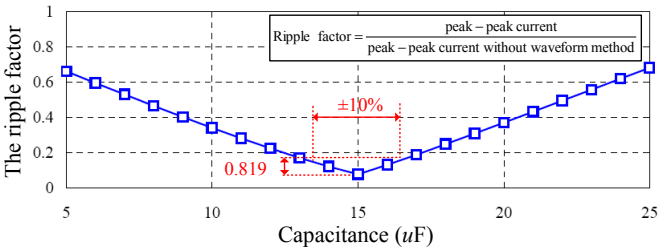

Fig. 4. Double-line-frequency current ripple factor versus capacitance of the inverter with waveform control designed under the assumption that $C_1 = C_2 = 15$ μF.

The specifications of the prototype are given in Table I. The control platform is implemented using TMS320LF2812.

TABLE I
SPECIFICATIONS OF BOOST DIFFERENTIAL INVERTER

Input voltage V_{in}	90 V
Output voltage (RMS)	110 V
Rated power P_e	170 W
Fundamental frequency f	50 Hz
Switch frequency f_s	20 kHz
Inductors (L_1, L_2)	300 μH, 10 A
Capacitors (C_1, C_2)	15 μF, 800 V, film cap.

In this work, the boost-inverter is based on a dual-loop control, of which each boost converter is controlled by means of an inner inductor current control loop and an outer output voltage control loop. An overview of the control block is shown in Fig. 5. Both control loops are designed using the averaged continuous-time model of the boost converter topology.

It is possible for the output of the differential inverter to contain a DC offset component due to control time delays and practical imperfections. Such an offset is prohibited and should be minimized when the inverter is to be connected to the grid [7]. In this work, the DC offset voltage compensation loop is included in the control, as shown in the control block given in Fig. 5. By introducing a DC current control loop into the controlled system, the DC offset voltage of the output will be regulated to zero. The control block diagram in Fig. 5 including the digital PI controller is implemented using the DSP unit TMS320LF2812.

B. Comparative Study of Waveform Control Versus No Waveform Control with Circuit Modification

As mentioned, without waveform control, the double-line-frequency current component will not flow through the capacitors C_1 and C_2. Therefore, a change in their capacitance values will not affect the current ripple. Consequently, the mitigation of the double-line-frequency component of the input current of the inverter without waveform control can be achieved only through the application of an extra device (e.g. by inserting an input capacitor to the inverter) or the use of an auxiliary converter that can alter the flow path of this component.

In this subsection, a comparative study on the addition of an input capacitor to the inverter without waveform control as compared to the use of waveform control is performed. Here, the double-line-frequency ripple levels under various configurations are performed. With the same capacitances $C_1 = C_2 = 15\mu$F and the same load ($R = 70.5$ Ω), the output voltage and input current waveform of the inverter for four separate cases are given in Fig.6. The configurations of the four cases are – Case I: without waveform control (no input capacitor); Case II: without waveform control but with 220 μF input electrolytic capacitor; Case III: without waveform control but with 2240 μF input electrolytic capacitor; Case IV: with proposed waveform control (no input capacitor).

From Fig.6, it is shown that the output voltage v_o can be controlled as sinusoidal, however, the peak-to-peak (double-line-frequency com-

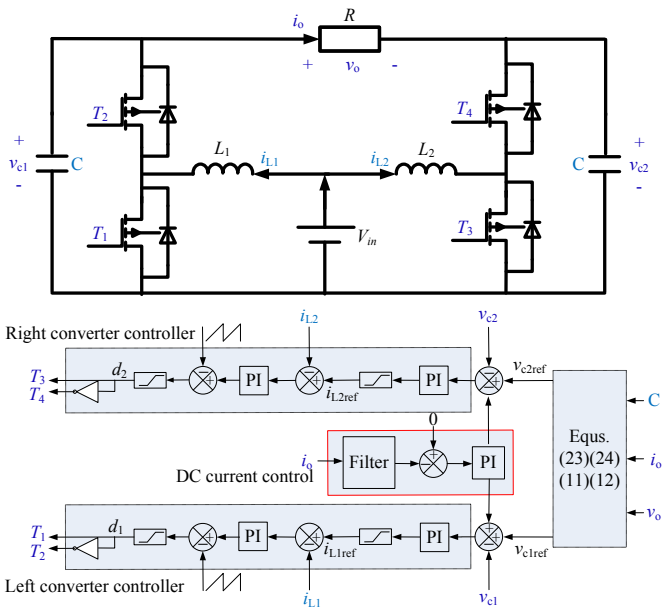

Fig. 5. Overview of the control block diagram of the differential inverter.

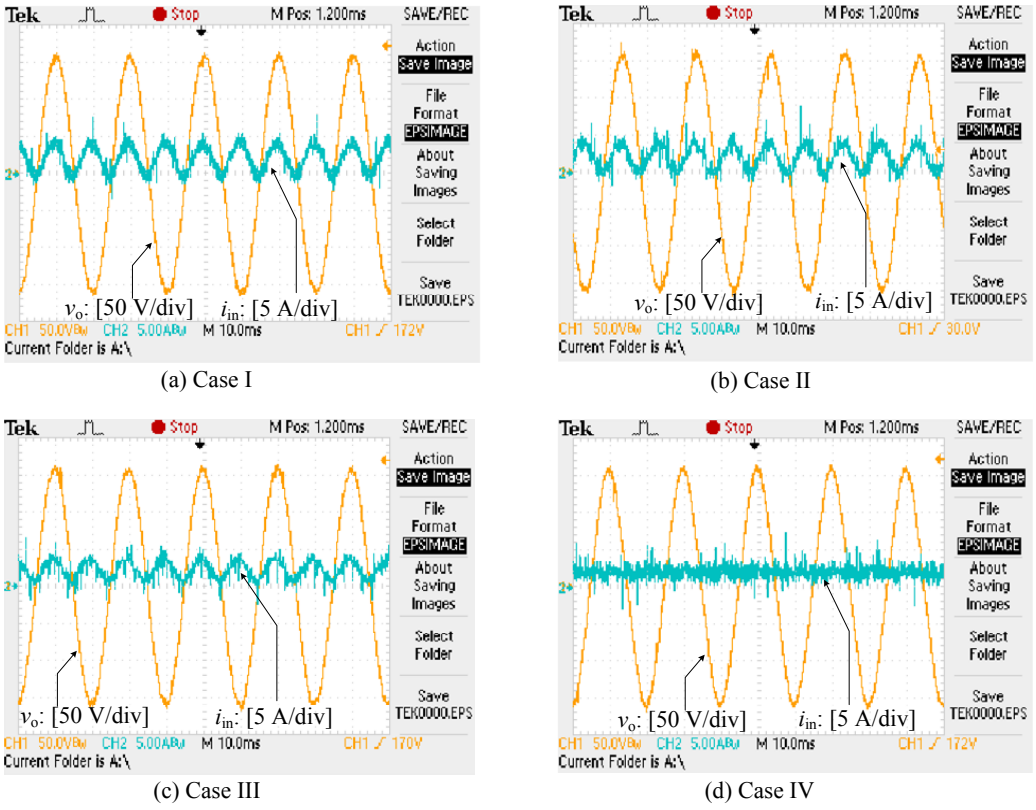

Fig. 6. Input current waveform in four cases. (a) Case I: without waveform control; (b) Case II: without waveform control but with 220 μF input capacitor; (c) Case III: without waveform control but with 2240μF input capacitor; and (d) Case IV: with waveform control.

ponent) of the input current is respectively 4 A, 3.8 A, 3.4 A, and 0.5 A in the four cases. With the same set of C_1 and C_2 values, the

use of the proposed waveform control method produces the minimal current ripple. The input current ripple is mitigated to a magnitude of less than 13% (from 4 A to 0.5 A) of the ripple magnitude that is obtained for the case of without waveform control (Case I). Additionally, without waveform control, the use of an input capacitor can help in suppressing the current ripple. However, the effect is not obvious and a very large electrolytic capacitor will be needed to achieve significant suppression.

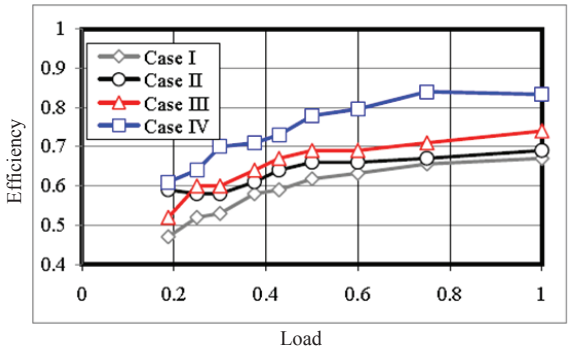

Fig. 7. The efficiency curves of the four cases. (a) Case I: without waveform control; (b) Case II: without waveform control but with 220 μF input capacitor; (c) Case III: without waveform control but with 2240μF input capacitor; and (d) Case IV: with waveform control.

Finally, the circuit efficiency curves for the four respective configuration obtained experimentally are given in Fig.7. From the Fig.7, it can be seen that power efficiency is higher with waveform control than without waveform control.

V. Conclusions

Assessment of Waveform Control Method for Mitigation of Low-Frequency Current Ripple is proposed in this paper. A comparative study on the waveform control and the traditional control method without waveform control is performed. It will be clearly illustrated in the paper that the waveform control solution achieves significant suppression of the low-frequency current ripple without any additional component, circuit, or electrolytic capacitor, therefore maintaining the overall size and cost. Additionally, the current stress of the switch is decreased and the total efficiency is improved with the use of waveform control.

References

[1] M. Schenck, J. S. Lai, and K. Stanton, "Fuel cell and power conditioning system interactions," in *IEEE APEC*, vol. 1, pp. 114–120, Jun. 2005.

[2] C. Liu and J. S. Lai, "Low frequency current ripple reduction technique with active control in a fuel cell power system with inverter load," *IEEE Trans. Power Electron.*, vol. 22, no. 4, pp. 1429–1436, Jul. 2007.

[3] Y. J. Song, S. B. Han, X. Li, S. I. Park, H. G. Jeong, and B. M. Jung. "A power control scheme to improve the performance of a fuel cell hybrid power source for residential application," in *Proc. IEEE PESC*, 2007, pp. 1261–1266.

[4] G. R. Zhu, S. C. Tan, K. W. Wang and Chi K. Tse, "Waveform Control of Fuel-cell Inverter Systems," in *Proc. IEEE ECCE*, 2011.

[5] M. Jang and V. G. Agelidis, "A minimum power-processing stage fuel cell energy system based on a boost-inverter with a bi-directional back-up battery storage," *IEEE Trans. Power Electron.*, vol. 26, no. 5, pp. 1568–1577, Dec. 2011.

[6] M. Jang, M. Ciobotaru and V. G. Agelidis, "A single-stage fuel cell energy system based on a buck–boost inverter with a backup energy storage unit," *IEEE Trans. Power Electron.*, vol. 27, no. 6, pp. 2825–2834, Dec. 2012.

[7] M. Armstrong, D. J. Atkinson, C. M. Johnson, and T. D. Abeyasekera, "Auto-calibrating DC link current sensing technique for transformerless, grid connected, H-bridge inverter systems," *IEEE Trans. Power Electron.*, vol. 21, no. 5, pp. 1385–1393, Sep. 2006.